


ORIGINAL ARTICLE

Procyanidin B2 inhibits the activation of hepatic stellate cells and angiogenesis via the Hedgehog pathway during liver fibrosis

Jiao Feng^{1,2} | Chengfen Wang¹ | Tong Liu² | Jingjing Li¹ | Liwei Wu² | Qiang Yu^{2,3} | Sainan Li² | Yuting Zhou^{2,3} | Jie Zhang^{2,3} | Jiaojiao Chen^{2,3} | Jie Ji² | Kan Chen² | Yuqing Mao⁴ | Fan Wang⁵ | Weiqi Dai^{1,2,6,7} | Xiaoming Fan⁸ | Jianye Wu¹ | Chuanyong Guo² 

¹Department of Gastroenterology, Putuo People's Hospital, Tongji University School of Medicine, Shanghai, China

²Department of Gastroenterology, Shanghai Tenth People's Hospital, Tongji University School of Medicine, Shanghai, China

³Shanghai Tenth Hospital, School of Clinical Medicine of Nanjing Medical University, Shanghai, China

⁴Department of Gerontology, Shanghai General Hospital, Shanghai Jiaotong University School of Medicine, Shanghai, China

⁵Department of Oncology, Shanghai General Hospital, Shanghai Jiaotong University School of Medicine, Shanghai, China

⁶Department of Gastroenterology, Zhongshan Hospital of Fudan University, Shanghai, China

⁷Shanghai Institute of Liver Diseases, Zhongshan Hospital of Fudan University, Shanghai, China

⁸Department of Gastroenterology, Jinshan Hospital of Fudan University, Jinshan, Shanghai, China

Correspondence

Jianye Wu, Department of Gastroenterology, Putuo People's Hospital, No. 1291, Jiangning Road, Putuo District, Shanghai 200072, China.
Email: wjymail@163.com and

Chuanyong Guo, Department of Gastroenterology, Shanghai Tenth People's Hospital, No. 301, middle Yanchang Road, Jing'an District, Shanghai 200072, China.
Email: guochuanyong@hotmail.com

Funding information

Natural Science Foundation of Shanghai, Grant/Award Number: 19ZR1447700

Abstract

Background: Liver fibrosis is a wound-healing process of liver featured by the over-deposition of extracellular matrix (ECM) and angiogenesis. However, the effective treatment is lacking. Procyanidin B2 (PB2) is a flavonoid extract abundant in grape seeds with anti-oxidant, anti-inflammatory and anti-cancer properties. The present study aimed to determine effects of PB2 on liver fibrosis.

Method: The CCl₄-induced mouse liver fibrosis model and a human hepatic stellate cell (HSC) line (LX2 cells) were used to study the activation, ECM production and angiogenesis of HSCs through Western blotting analysis, immunohistochemistry, immunofluorescence staining, flow cytometry and tubulogenesis assay. A Hedgehog (Hh) pathway inhibitor (cyclopamine) and Smoothed agonist (SAG) were used to investigate the role of PB2 on Hh pathway.

Results: The results showed that PB2 could inhibit the proliferation and induce apoptosis of HSCs. PB2 could also down-regulate the expressions of VEGF-A, HIF-1 α , α -SMA, Col-1 and TGF- β 1 of HSCs in vivo and in vitro. The application of SAG and cyclopamine proved that PB2 targets on Hh pathway.

Feng and Wang contributed equally.

This is an open access article under the terms of the Creative Commons Attribution License, which permits use, distribution and reproduction in any medium, provided the original work is properly cited.

© 2019 The Authors. *Journal of Cellular and Molecular Medicine* published by John Wiley & Sons Ltd and Foundation for Cellular and Molecular Medicine.

Conclusions: PB2 inhibited the Hh pathway to suppress the activation, ECM production and angiogenesis of HSCs, therefore reverses the progression of liver fibrosis *in vivo* and *in vitro*.

KEYWORDS

angiogenesis, Hedgehog pathway, hepatic stellate cells, liver fibrosis, procyanidin B2

1 | INTRODUCTION

Liver fibrosis is a wound-healing process of the liver in response to repeated and chronic liver injuries, including viral infection, cholestatic liver disease, alcohol abuse, non-alcoholic steatohepatitis, non-alcoholic fatty liver disease and the side effects of some drugs.¹⁻³ It is characterized by the excessive deposition of extracellular matrix (ECM) and formation of fibrous scar, giving rise to hepatic dysfunction and the possible progression to liver cirrhosis and hepatocellular carcinoma.⁴ Fortunately, liver fibrosis is a reversible process if the primary causative factors are removed, but this is always difficult and time-consuming. Currently, the most effective therapeutic treatment for liver fibrosis is liver transplantation.³ Liver transplantation is not available and popular, however, because of the limitation of organ donors. Therefore, there is need to identify a new agent for the treatment of liver fibrosis to relieve liver dysfunction and decrease complications.

The pathogenesis of liver fibrosis has recently been well-described, and hepatic stellate cells (HSCs) activation is the critical stage.^{4,5} In healthy livers, HSCs are liver mesenchymal cells that are responsible for vitamin A storage. HSCs are localized in Disse's space and have a quiescent phenotype (qHSCs); however, when the liver is challenged with an injury stimulus, the Kupffer cells and other mesenchymal cells are activated and secrete various fibrogenic cytokines, including transforming growth factor-beta 1 (TGF- β 1), platelet-derived growth factor (PDGF) and epidermal growth factor (EGF), which result in the activation of HSCs.⁵ The activated phenotype of HSCs (aHSCs) then undergoes a cascade of activation responses, leading to the production of excessive ECM and fibrogenesis.

Except for the deposition of ECM, liver injury is associated with angiogenesis. Further, angiogenesis and fibrogenesis always develop in parallel with chronic liver disease because of tissues hypoxia.^{6,7} Pathological angiogenesis exacerbates structure turbulence instead of providing relief. It has been reported that inhibition of angiogenesis by tyrosine kinase inhibitors, such as sunitinib or sorafenib, improves liver fibrosis in rodents.^{8,9} Hence, angiogenesis is also an important target for the treatment of liver fibrosis.

Procyanidins are a type of flavonoid that are widespread in red wine, green and black tea, cocoa/chocolate, and fruit juices.^{10,11} Procyanidins have been shown to possess anti-oxidant, anti-tumour, anti-inflammatory, anti-allergic, and cardiovascular and brain protection properties.¹²⁻¹⁴ Among the procyanidins, a B-type procyanidin dimer, procyanidin B2 (PB2), has been shown to possess greater anti-oxidant and anti-tumour effects than other PAs, such as procyanidin B1, B4 and B5.^{15,16} Therefore, the special bioactivities

of PB2 aroused our interest. Justino et al have reported that the *Annona crassiflora* fruit peel extract, which contains PB2, exhibits hepatoprotective properties.¹⁷ Yang et al showed that PB2 can protect against carbon tetrachloride (CCl₄)-induced acute liver injury in mice via suppression of the inflammatory response and apoptosis.¹⁸ There are few studies involving the effects of PB2 on chronic liver injuries, including the underlying mechanism of action.

The Hedgehog (Hh) pathway is responsible for embryogenesis, development and tissue remodelling.¹⁹ The Hh pathway plays an important role during various liver injuries, such as liver fibrosis, inflammation-related injury and liver carcinogenesis.^{6,20} Activation of HSCs and angiogenesis is associated with the Hh signalling pathway.^{1,21} Targeting the Hh pathway has become a promising treatment for liver fibrosis.¹ Therefore, the study was designed to examine the effects of PB2 on liver fibrosis, with particular attention to the activation of HSCs, angiogenesis and the Hh pathway.

2 | MATERIALS AND METHODS

2.1 | Reagents

PB2, pentobarbital sodium salt, cyclopamine hydrate and Smoothed agonist (SAG) were purchased from Sigma-Aldrich (Merck KGaA). Sorafenib tosylate was purchased from Selleck Chemicals. CCl₄ was purchased from China Sinopharm International Corporation. TGF- β 1 was obtained from PeproTech. Alanine aminotransferase (ALT), aspartate aminotransferase (AST) and hydroxyproline detection kits were purchased from Nanjing Jiancheng Bioengineering Institute. Oligonucleotide primers were synthesized by Generay Biotech Co., Ltd. The PrimeScript RT Reagent kit and SYBR Premix Ex Taq were purchased from TaKaRa Biotechnology. The primary antibodies used in the study are listed in Table 1. Anti-goat or antimouse secondary antibodies were obtained from Dako. Dulbecco's Modified Eagle Medium (DMEM) and foetal bovine serum (FBS) were from HyClone (GE Healthcare). The Annexin V-FITC apoptosis detection kit was purchased from BD Biosciences. Growth factor-reduced Matrigel was purchased from BD Biosciences. PB2, sorafenib and cyclopamine were dissolved in DMSO (<0.1% [v/v]) for *in vitro* treatment.

2.2 | Animals and establishment of CCl₄-induced liver fibrosis model

Six-week-old male C57 mice weighing 24 ± 2 g were purchased from Shanghai SLAC Laboratory Animal Co., Ltd. and kept in

TABLE 1 The primary antibodies used in the study

Antibody	Species	Targeted species	Dilution ratio	Supplier	Catalogue number
HIF-1 α	R	H	1:1000	PT	20960-1-AP
HIF-1 α	M	H, M	1:1000	Abcam	ab113642
α -SMA	R	H, M	1:1000	PT	14395-1-AP
Col-1	R	H, M	1:1000	PT	14695-1-AP
CD31	R	H, M	1:500	Abcam	ab28364
VEGF-A	M	H, M	1:1000	Abcam	ab1316
SMO	R	H, M	0.1-1 μ g/mL	Abcam	ab72130
GLI1	M	H	1:1000	CST	2643
GLI1	R	H, M	1:1000	Abcam	ab151796
β -actin	M	H, M, R	1:1000	CST	3700
TGF- β 1	R	H, M, R	1:500	BT	BS1361

Abbreviations: H, human; M, mouse; R, rabbit; CST, Cell Signaling Technology (Danvers, MA, USA). PT (Chicago, IL, USA). Abcam (Cambridge, MA, USA). BT, Bioworld Technology (St. Louis Park, MN, USA).

environmentally controlled conditions with free access to standard laboratory chow and water. The experiments were approved by the Animal Care and Use Committee of Shanghai Tongji University and conducted following the ARRIVE Guidelines. Forty-two mice were randomly divided into seven groups ($n = 6$), as follows: (a) normal control (NC) group, no treatment; (b) vehicle group, injected with peanut oil intraperitoneally only; (c) PB2 group, treated with 150 mg/kg of PB2 by gavage during the 5th-8th weeks; (d) CCl₄ group, injected with CCl₄; and (e-g) L, M and H groups, respectively, treated with CCl₄ and PB2 (50, 100 and 150 mg/kg, respectively).¹⁸ The CCl₄-induced liver fibrosis model was established according to previous studies.²²⁻²⁶

To further investigate the effect of PB2 on Hh pathway in vivo, another 20 mice were induced by CCl₄ to establish the liver fibrosis model and then randomly divided into four groups ($n = 5$): (a) CCl₄ group; (b) PB2(M) group, treated with PB2 100 mg/kg by gavage during the 5th-8th weeks; (c) cyclopamine group, treated with cyclopamine 30 mg/kg by gavage during the 5th-8th weeks⁶; (d) PB2 + cyclopamine group, treated with PB2 100 mg/kg and cyclopamine 30 mg/kg during the 5th-8th weeks.

Twenty-four hours after the last treatment, all of the mice were anaesthetized with pentobarbital intraperitoneally. Blood samples were collected and kept at -80°C . Some of the liver tissues were cut and stored at -80°C ; other tissue samples were immersed in 4% paraformaldehyde.

2.3 | Cell culture and CCK8 assay

The human immortal LX2 cell line was cultured in high glucose DMEM with 10% FBS, 100 U/mL of penicillin and 100 g/mL of streptomycin. The apparent logarithmic phase cells were seeded in 96-well plates for 48 hours, then PB2 was added at concentrations of 10, 20, 40, 80, 160 or 320 μM for 24 hours, and the cytotoxicity analysis was performed. Cell viability was then measured with the CCK8 assay. The in vitro experiments were conducted using the following four groups: (a) NC group, LX2 cells without any treatment; (b-d) L, M and H groups, respectively, LX2 cells were treated with 60, 80 and 100 μM

PB2, respectively; (e) cyclopamine group, LX2 cells were treated with 10 μM cyclopamine⁶; and (f) PB2 (M) + SAG group, LX2 cells were treated with 100 nM SAG.^{27,28} All of the experiments were performed in triplicate.

2.4 | Flow cytometry analysis

Cells were seeded in 6-well plates for 48 hours and then treated with different concentrations of PB2 for 24 hours. The Annexin V-FITC/PI apoptosis detection kit and a flow cytometer (Beckman Coulter, Inc) were used for detection of cell apoptosis. Annexin V-FITC positive (with or without PI-positive) cells were regarded as apoptotic (early-phase or late phase) cells using the FlowJo software (version 10; FlowJo LLC).

2.5 | Biochemical assays

Detection of serum ALT, AST and liver hydroxyproline concentrations were determined according to the manufacturer's protocols.

2.6 | Histopathology

Paraformaldehyde-immersed liver tissues were embedded in paraffin and cut into 3- μm thick sections. For haematoxylin and eosin (H & E) staining, the slices were stained with H for 10 minutes and E for 5 minutes to demonstrate the liver injuries. Masson's trichrome and Sirius Red staining were used according to previous studies.^{25,29} Five random fields of view for each slice were captured and analysed in the experiment.

2.7 | Reverse transcription-polymerase chain reaction and quantitative real-time PCR

The total RNA from LX2 cells was extracted by TRIzol, and reverse transcription-polymerase chain reaction (RT-PCR) was performed. The primers used for quantitative real-time PCR (qRT-PCR) are listed in

Genes name	Forward (5'-3')	Reverse (5'-3')
α -SMA	AAAAGACAGCTACGTGGGTGA	GCCATGTTCTATCGGGTACTTC
Col-1 α 1	GAGGGCCAAGACGAAGACATC	CAGATCACGTCATCGCACAAAC
Col-1 α 2	GTTGCTGCTTGCAGTAACCTT	AGGGCCAAGTCCAACCTCCTT
TGF- β 1	GGCCAGATCCTGTCCAAGC	GTGGGTTTCCACCATTAGCAC
VEGF-A	AGGGCAGAATCATCACGAAGT	AGGGTCTCGATTGGATGGCA
SMO	GAAGTGCCTTGTTTCGGA	GCAGGGTAGCGATTTCGAGTT
GLI1	AGCGTGAGCCTGAATCTGTG	CAGCATGTACTGGGCTTTGAA
HIF-1 α	GAACGTCGAAAAGAAAAGTCTCG	CCTTATCAAGATGCGAACTCACA
β -actin	CATGTACGTTGCTATCCAGGC	CTCCTTAATGTCACGCACGAT

TABLE 2 Primers used in the study

Table 2 and were determined using a 7900HT Fast PCR System (Applied Biosystems). The results were quantified using the $2^{-\Delta\Delta Ct}$ method.³⁰

anti-fluorescence quenching sealant and observed with an inverted fluorescence microscope (Leica DMIRB).

2.8 | Western blot analysis

Total protein was extracted using RIPA lysis buffer and quantified with a BCA kit. Eighty micrograms of protein were loaded per well on 7.5%-12.5% SDS-PAGE for electrophoresis, then transferred to PVDF membranes and blocked with 5% non-fat milk, following by incubation with primary antibodies overnight. The next day, the membranes were incubated with secondary antibodies and detected using Odyssey (Licor). Quantitative analysis of Western blots was conducted by ImageJ software.

2.9 | Immunohistochemistry staining

After dewaxed and rehydrated, the sections were performed with an antigen retrieval technique. About 3% hydrogen peroxide and 5% BSA were used to block the endogenous and non-specific binding sites. Then, the slices were incubated with primary antibodies at 4°C. The next day, slides were incubated with secondary antibody and then counterstained with H&E and observed. The brown-stained cells were regarded as positive cells, and the positive rates were calculated using Image-Pro Plus software 6.0.

2.10 | Immunofluorescence staining

The treated LX2 cells slices were fixed with 4% paraformaldehyde and incubated with primary antibodies against α -SMA, VEGF-A or GLI1 at 4°C. The next day, the slices were incubated with fluorescence secondary antibody and DAPI, and then mounted with

2.11 | Tubulogenesis assay

The tubulogenesis assay was designed with the guidance of a previous study.⁶ Briefly, the NC, PB2 (M), Sora and PB2 + Sora groups of LX2 cells were pretreated with related drugs for 24 hours and starved for 8 hours before use. Fifty microlitres of growth factor-reduced Matrigel were added to 96-well plates and placed in a 37°C incubator for 30 minutes. Then, the pretreated LX2 cells were resuspended with FBS-free DMEM and added to the Matrigel at a density of 2×10^4 /well. The results were observed and captured by microscopy at 2, 3, 4, 5, 6, 8, 10 and 24 hours after seeding.

2.12 | Statistical analysis

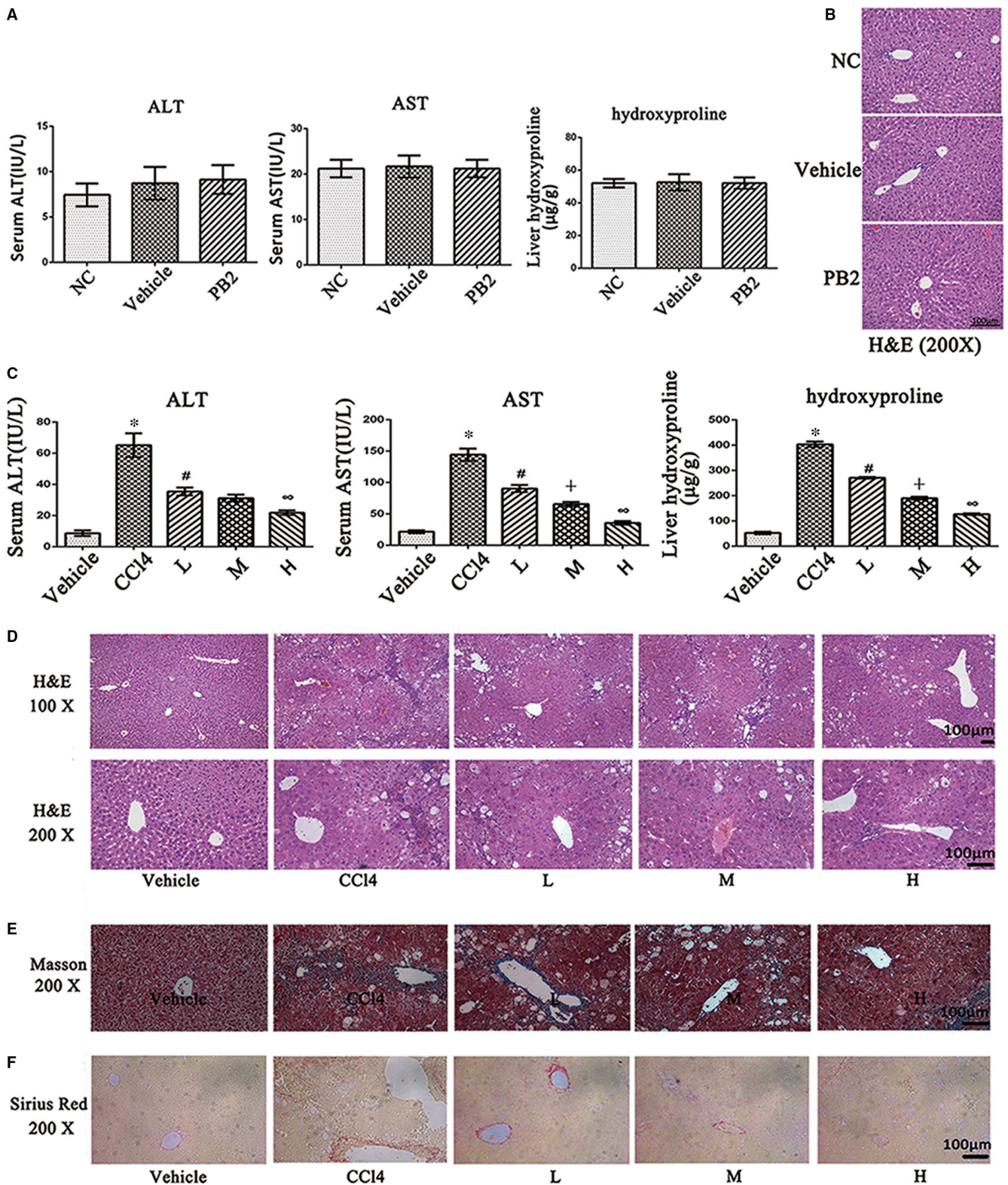
All data are reported as mean \pm standard deviation (SD) and imaged using GraphPad Prism 6 software (GraphPad Software). The results were analysed with Student's *t* test and one-way analysis of variance, followed by Tukey's post hoc test. Statistically significance was defined as $P < .05$.

3 | RESULTS

3.1 | PB2 has no toxicity on liver function and liver pathology

To study the toxicity of PB2 and vehicle oil on liver, we conducted a preliminary study to examine the safety of PB2 on liver function in mice. As shown in Figure 1A, the serum ALT and AST levels, which

FIGURE 1 Effects of PB2 on CCl₄-induced liver fibrosis in mice. A, The serum ALT and AST levels and liver hydroxyproline concentrations. Data are presented as the mean \pm SD ($n = 6$, from three independent experiments). B, The H & E staining of liver tissues in the NC, vehicle and PB2 groups (original magnification, 200 \times). The structures were clear, and the hepatocytes were well-preserved with clear cytoplasm and prominent nuclei and nucleoli. C, The serum ALT and AST levels and liver hydroxyproline concentrations. Data are presented as the mean \pm SD ($n = 6$, from three independent experiments). * Indicates $P < .05$ vs the vehicle group; # indicates $P < .05$ vs the CCl₄ group; † indicates $P < .05$ vs the L group; ∞ indicates $P < .05$ vs the M group (D) The H & E staining of liver tissues (original magnification, 100 \times and 200 \times). There was a rearrangement of liver lobular structures, a formation of peri-cellular collagen deposition, and diffuse swelling of hepatocytes and infiltration of inflammatory cells in the CCl₄ group. PB2 can effectively relieve the pathologic injuries. E, Masson's trichrome staining of liver tissues. The blue-stained areas referred to ECM deposition (original magnification, 200 \times). F, Sirius Red staining of liver tissues. The red-stained areas indicated type I collagen deposition (original magnification, $\times 200$)



are usually regarded as biomarkers of liver injury, were not elevated in the vehicle and PB2 (150 mg/kg) groups when compared to the NC group. The liver hydroxyproline concentration, which is used as an indirect measurement of tissue collagen content, did not differ between these three groups as well. H&E staining of liver slices in

the three groups revealed normal morphology (Figure 1B). These results indicated that vehicle oil and PB2 (at the highest test concentration) had no toxic effects on liver function and liver pathology. Therefore, the vehicle group served as the control group in subsequent animal experiments.

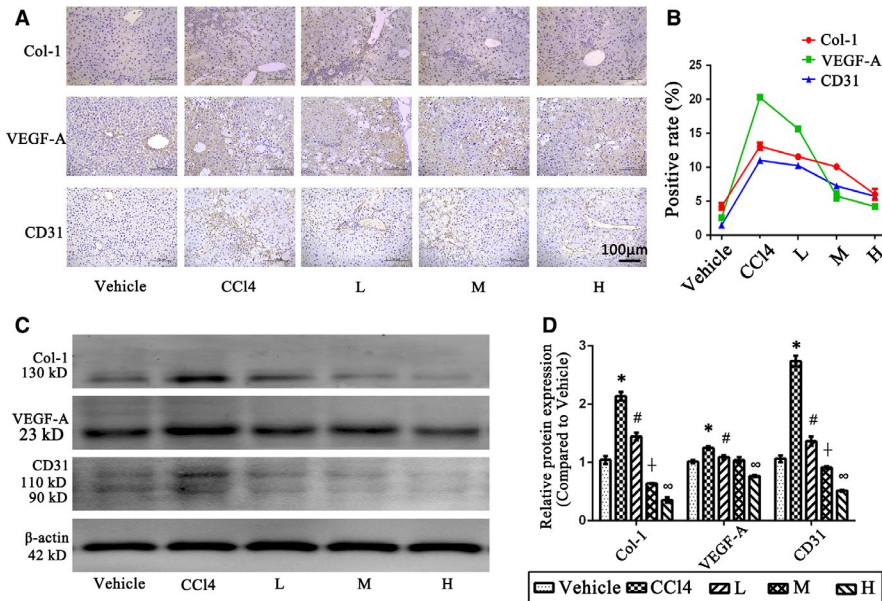


FIGURE 2 Effect of PB2 on the ECM deposition and angiogenesis in CCl₄-induced liver fibrosis tissues. A, IHC staining of Col-1, VEGF-A and CD31 in liver tissues (original magnification, 200×). The brown-stained areas were considered to be positive. B, The quantitative analysis of IHC results. C & D, The expression of Col-1, VEGF-A and CD31 protein in liver tissues and the quantitative analysis of Western blot results. Data are presented as the mean ± SD (n = 6, from three independent experiments). * indicates $P < .05$ vs the vehicle group; # indicates $P < .05$ vs the CCl₄ group, † indicates $P < .05$ vs the L group and ∞ indicates $P < .05$ vs the M group

3.2 | PB2 relieves liver injury and fibrogenesis in CCl₄-induced liver fibrosis in mice

Because PB2 is safe, we then established a CCl₄-induced liver fibrosis murine model to determine the effect of PB2 in liver fibrosis. The results in Figure 1C show that the serum levels of ALT and AST were dramatically elevated in the CCl₄ group when compared to the vehicle group with respect to the occurrence of liver injuries. The liver hydroxyproline concentration was also increased in the CCl₄ group; however, treatment of PB2 effectively reduced the levels of liver enzymes and hydroxyproline in a dose-dependent manner. The H&E staining showed that in the vehicle group, the liver tissues were well-constructed and the hepatocytes were well-preserved with clear cytoplasm and a prominent nucleus and nucleolus. In the CCl₄ group, normal liver structure was replaced by a rearrangement of liver lobular structures and a formation of peri-cellular collagen deposition. There was diffuse swelling of hepatocytes and infiltration of inflammatory cells. PB2 treatment also reduced the pathological changes of liver tissues (Figure 1D). Masson's trichrome and Sirius Red staining, which are used to detect collagen deposition, also revealed the same results as H&E staining (Figure 1E,F). These results confirmed the successful establishment of a liver fibrosis model and indicated that PB2 treatment can attenuate liver fibrogenesis in mice in a dose-dependent manner.

3.3 | PB2 inhibits the angiogenesis during liver fibrosis

As reported, angiogenesis is a remarkable pathological manifestation of liver fibrosis and always develops in parallel with fibrogenesis in chronic liver disease.^{6,7} We used immunohistochemistry (IHC) staining to detect the expression of Col-1 (a vital marker for ECM deposition), VEGF-A (an effective cytokine that promotes angiogenesis) and CD31 (a marker for the formation of new vessels) in liver

tissues. As shown in Figure 2A,B, the expression of Col-1, VEGF-A and CD31 was limited in the vehicle group, and the positive rate of these three markers was higher in the CCl₄ group. Thus, there was significant ECM deposition and angiogenesis in the liver fibrosis model, and the statistical analysis of IHC staining in Figure 2B confirmed that angiogenesis was positively correlated with fibrogenesis. In the PB2 treatment groups, the IHC positive rates of Col-1, VEGF-A and CD31 were significantly reduced in a dose-dependent fashion. Western blot analysis of liver tissues also demonstrated the same results as IHC staining (Figure 2C,D). Overall, these results showed that PB2 ameliorated fibrogenesis and angiogenesis in liver tissues.

3.4 | PB2 suppresses proliferation and activation, and promotes apoptosis of LX2 cells

To further investigate the protective mechanism of PB2 in liver fibrosis, a human immortal HSC cell line (LX2 cells) was used in this study. The CCK8 assay was used to measure the toxicity of PB2 in LX2 cells (Figure 3A). PB2 inhibited the viability of LX2 cells in a dose-dependent manner, and the half-maximal inhibitory concentration (IC₅₀) was 82.56 μM. In a subsequent in vitro experiment, 60, 80 and 100 μM of PB2 were used as a different concentration gradient to treat LX2 cells and defined as the L, M and H groups, respectively. Flow cytometry analysis of apoptosis in Figure 3B,C showed that PB2 promoted apoptosis the LX2 cells. Via the inhibition of proliferation and promotion of apoptosis, the number of LX2 cells was decreased. The activation of HSCs by TGF-β1 is an important process during fibrogenesis, leading to the excessive production of ECM. The qRT-PCR and Western blot results showed that the expression of α-SMA (a marker of activated HSCs), Col-1, and TGF-β1 mRNA and protein was reduced in the L, M and H groups, indicating that PB2 treatment inhibited the activation and ECM production in HSCs (Figure 3D,E). The immunofluorescence (IF) stain of α-SMA in LX2 cells also confirmed inhibition of α-SMA

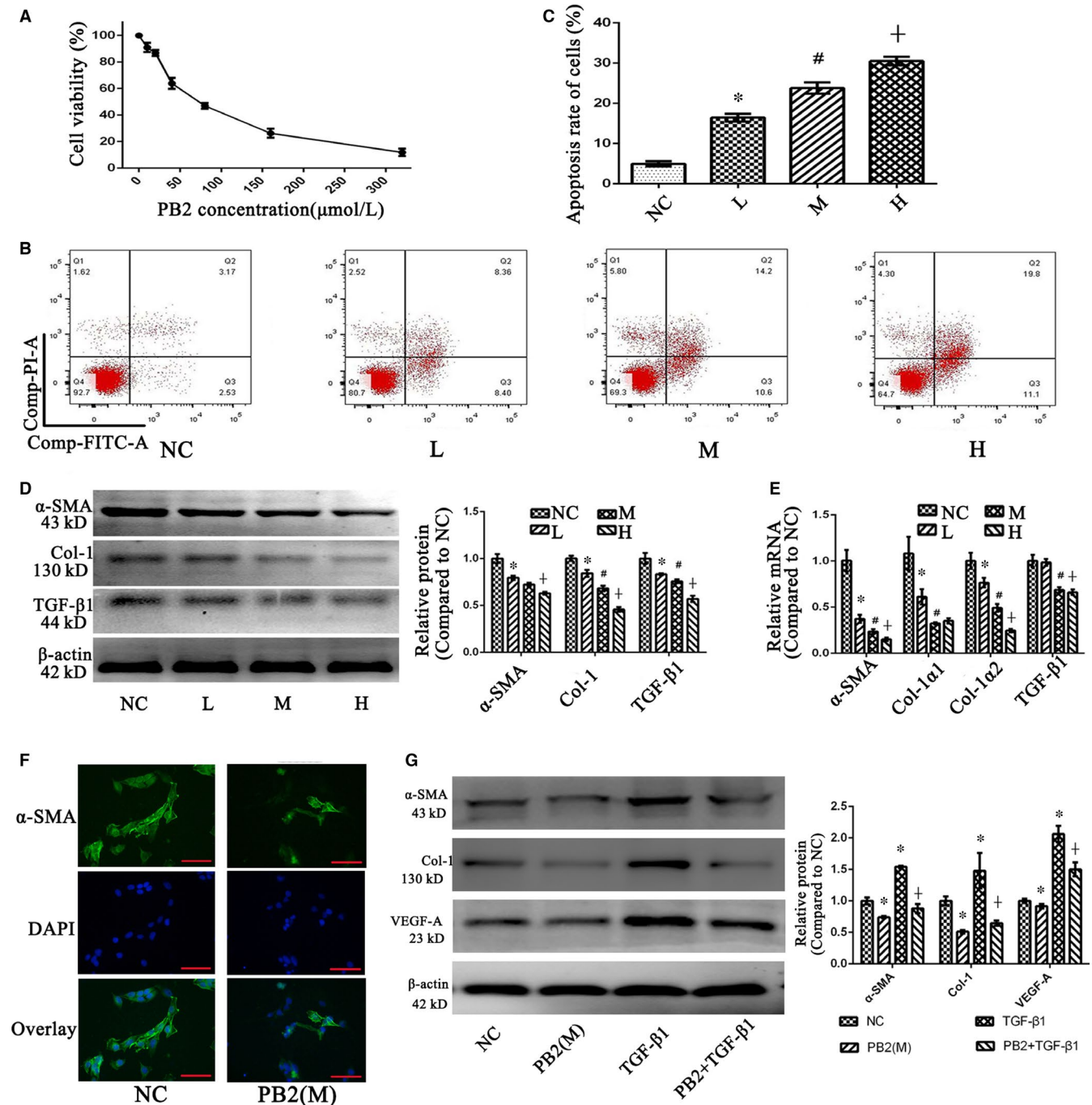


FIGURE 3 Effects of PB2 on the proliferation, apoptosis and activation of LX2 cells. A, The CCK8 assay was used to determine the effects of PB2 on the viability of LX2 cells. B & C, Flow cytometry detection of apoptosis and apoptosis rate of LX2 cells. D, The expression of α -SMA, Col-1 and TGF- β 1 protein in LX2 cells. E, The levels of α -SMA, Col-1 α 1, Col-1 α 2 and TGF- β 1 mRNA in LX2 cells. All of the experiments were repeated in triplicate. Data are presented as the mean \pm SD from three independent experiments. * Indicates $P < .05$ vs the NC group; # indicates $P < .05$ vs the L group; and † indicates $P < .05$ vs the M group. F, IF staining of α -SMA in LX2 cells in the NC and PB2 (M) groups (original magnification, $\times 400$; bar: 50 μ m). G, Effects of TGF- β 1 and PB2 co-treatment on LX2 cells' activation and angiogenesis. PB2 was effective to reverse the activation effect of TGF- β 1 on LX2 cells. * Indicates $P < .05$ vs the NC group; † indicates $P < .05$ vs the TGF- β 1 group

expression in HSCs, which was consistent with the qRT-PCR and Western blot results (Figure 3F). Moreover, to furtherly verify the role of PB2 during the inhibition of HSCs activation, exogenous TGF- β 1 (10 ng/mL) was used to activated LX2 cells.³¹ As the results

shown in Figure 3G, in TGF- β 1 treated group, the expression of α -SMA was enhanced in LX2 cells when compared to NC group, and PB2 treatment can inhibit the expression of α -SMA. However, if LX2 cells were administrated with both TGF- β 1 and PB2, then the

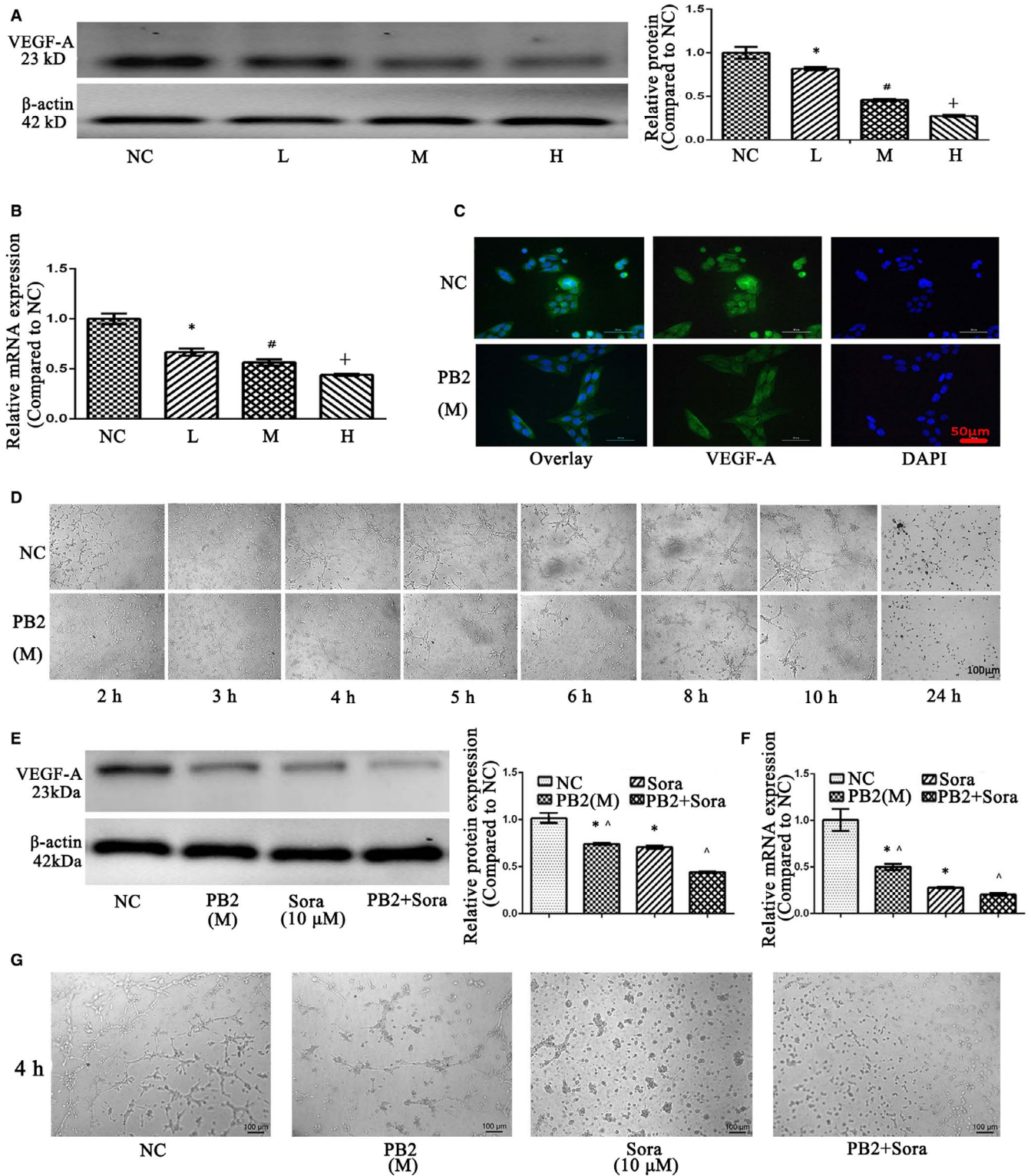


FIGURE 4 Effects of PB2 on the angiogenesis ability of LX2 cells. A, The expression of VEGF-A protein in LX2 cells. B, The levels of VEGF-A mRNA in LX2 cells. C, IF staining of VEGF-A in LX2 cells (original magnification, 400×). D, A tubulogenesis assay was used to detect the angiogenesis ability of LX2 cells (original magnification, 100×). PB2 inhibited the formation and size of closed rings or pro-angiogenic structures in LX2 cells. E, Effect of sorafenib on the protein expression of VEGF-A. F, Effect of sorafenib on the transcription of VEGF-A. G, Effect of sorafenib on the angiogenesis ability of LX2. All of the experiments were repeated in triplicate. Data are presented as the mean ± SD from three independent experiments. * Indicates $P < .05$ vs the NC group; # indicates $P < .05$ vs the L group; † indicates $P < .05$ vs the M group; and ^ indicates $P < .05$ vs the Sora group

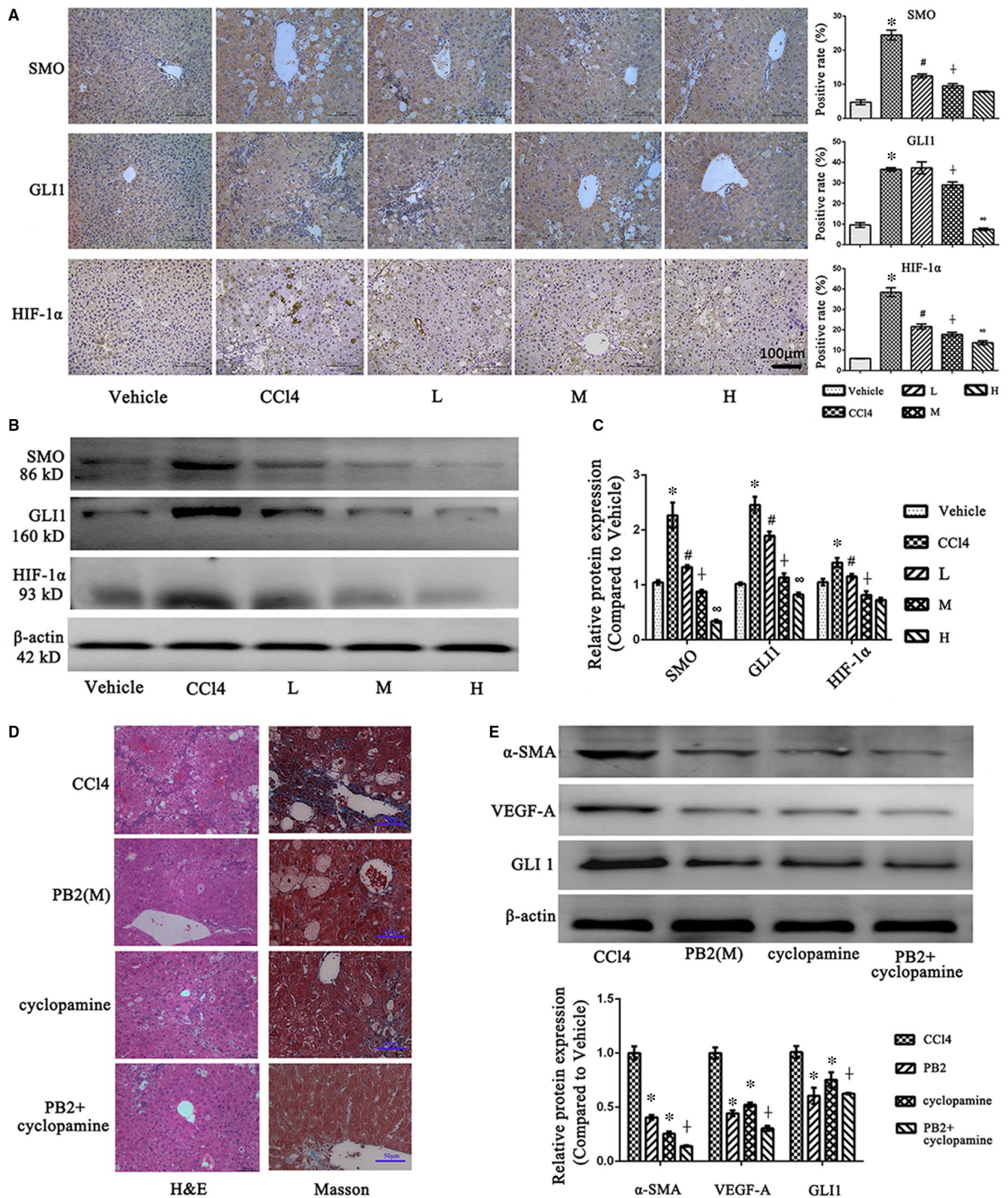


FIGURE 5 Effects of PB2 on the Hh pathway in CCI4-induced liver fibrosis in mice. A, IHC staining and quantitative analysis of SMO, GLI1 and HIF-1α in liver tissues (original magnification, ×200). B, The expression of SMO, GLI1 and HIF-1α protein in liver tissues. C, The quantitative analysis of Western blot results. Data are presented as the mean ± SD (n = 6, from three independent experiments). * Indicates $P < .05$ vs the vehicle group; # indicates $P < .05$ vs the CCI4 group; † indicates $P < .05$ vs the L group; and ∞ indicates $P < .05$ vs the M group. D, The H&E staining and Masson's trichrome staining of liver tissues after cyclopamine treatment in vivo. E, The Western blotting analysis of α-SMA, VEGF-A and GLI1 after cyclopamine treatment in vivo. Data are presented as the mean ± SD (n = 5). * Indicates $P < .05$ vs the CCI4 group; † indicates $P < .05$ vs the cyclopamine group

overexpression of α -SMA induced by TGF- β 1 can also be depressed, which indicated PB2 was effective to reverse the activation effect of TGF- β 1. The expression of Col-1 and VEGF-A was similar to α -SMA after both TGF- β 1 and PB2 treatment. These results declared that PB2 can suppress the proliferation and activation, and promote the apoptosis of LX2 cells.

3.5 | PB2 inhibits the angiogenesis ability of LX2 cells

Hepatic stellate cells have been shown to regulate angiogenesis during liver fibrosis by secreting strong stimuli of angiogenesis, such as VEGF-A, angiopoietin 1, placental growth factor and epidermal growth factor chemokine receptor 1.^{32,33} VEGF-A is the most potent stimulus and promotes the proliferation, migration, differentiation and tubulogenesis of vascular endothelial cells, thus giving rise to angiogenesis in liver fibrosis. Therefore, we used different concentrations of PB2 to treat LX2 cells and analysed the angiogenesis ability of HSCs. The Western blot and qRT-PCR results showed that the translation and transcription of VEGF-A were inhibited by PB2 treatment in a dose-dependent manner (Figure 4A,B). IF staining of VEGF-A in the NC and M groups also verified that the expression of VEGF-A was suppressed by PB2 in LX2 cells (Figure 4C). Moreover, the tubulogenesis assay, which can examine the angiogenesis ability of LX2 cells, revealed that the tubulogenesis ability of LX2 cells fluctuated with time and peaked at 5 hours in the NC group (Figure 4D). In the M group, however, PB2 treatment inhibited the tubulogenesis ability of LX2 cells, which was reflected by fewer and smaller, but earlier elimination of cavity formation.

To further verify the anti-angiogenesis ability of PB2, we used sorafenib, which can inhibit the neovascularization in liver cancers, to compare the angiogenesis inhibition effect between PB2 and sorafenib. The dosage of sorafenib was 10 μ M, which was determined according to previous studies.³⁴⁻³⁶ As the results shown in Figure 4E, the protein expression of VEGF-A was decreased in both PB2(M) and Sora group, and was much lower in the PB2 + Sora group. In Figure 4F, the qRT-PCR results are shown to be consistent with the Western blot results. In addition, the tubulogenesis assay in Figure 4G demonstrated that both PB2 and sorafenib inhibited the tubulogenesis ability of LX2 cells at 4 hours. These indicated that PB2 was as effective in inhibiting the angiogenesis process in LX2 cells as sorafenib, and the combined treatment of PB2 and sorafenib enhanced the angiogenesis inhibitory effect of sorafenib.

In conclusion, these results confirmed the angiogenesis ability of LX2 cells and indicated that PB2 effectively inhibited the angiogenesis ability of LX2 cells by suppressing the expression of VEGF-A and tubulogenesis.

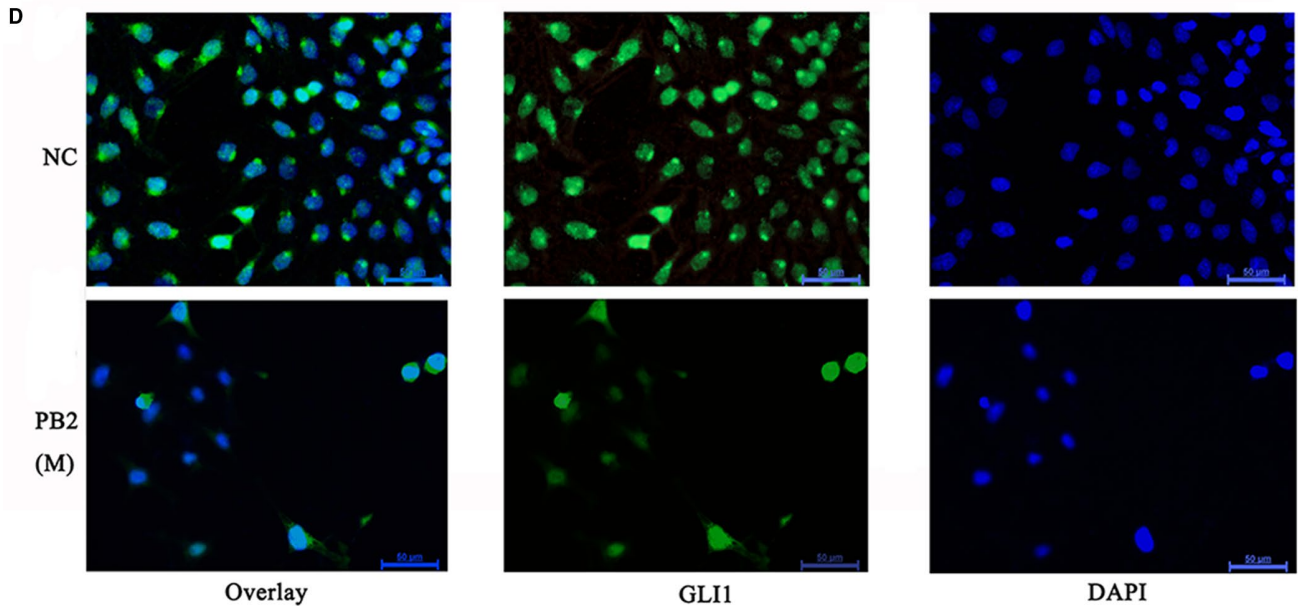
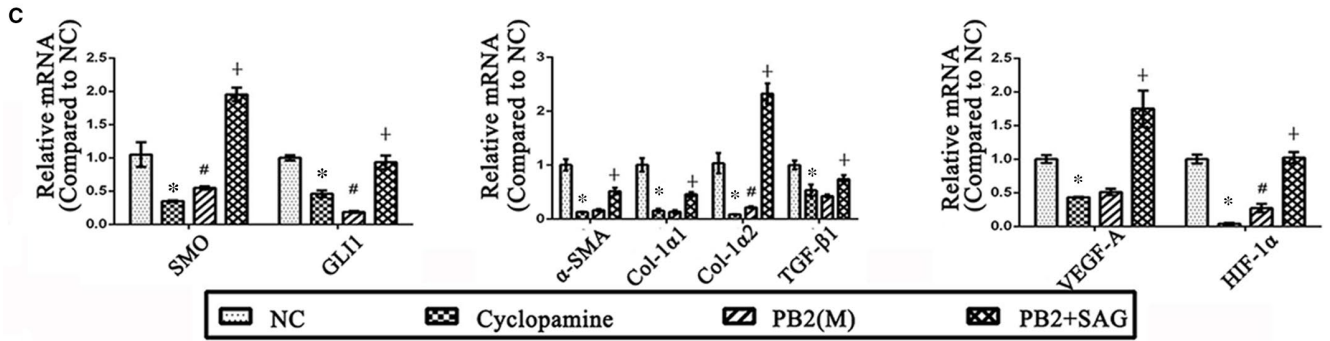
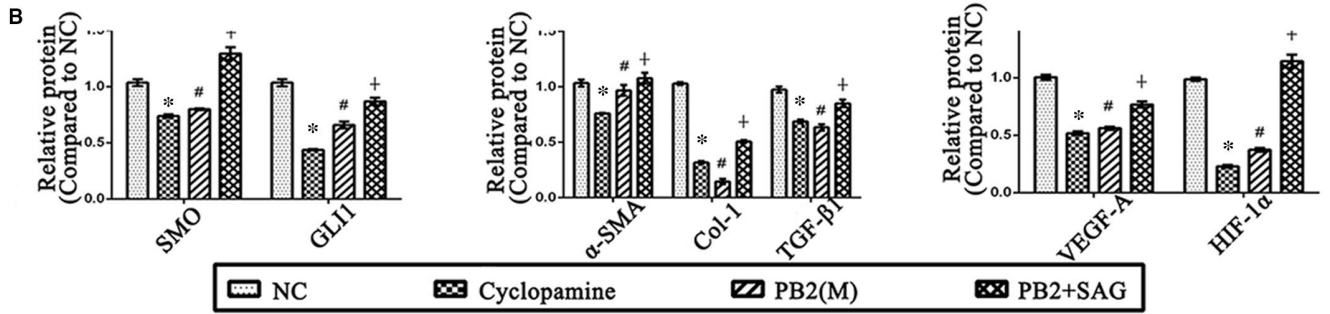
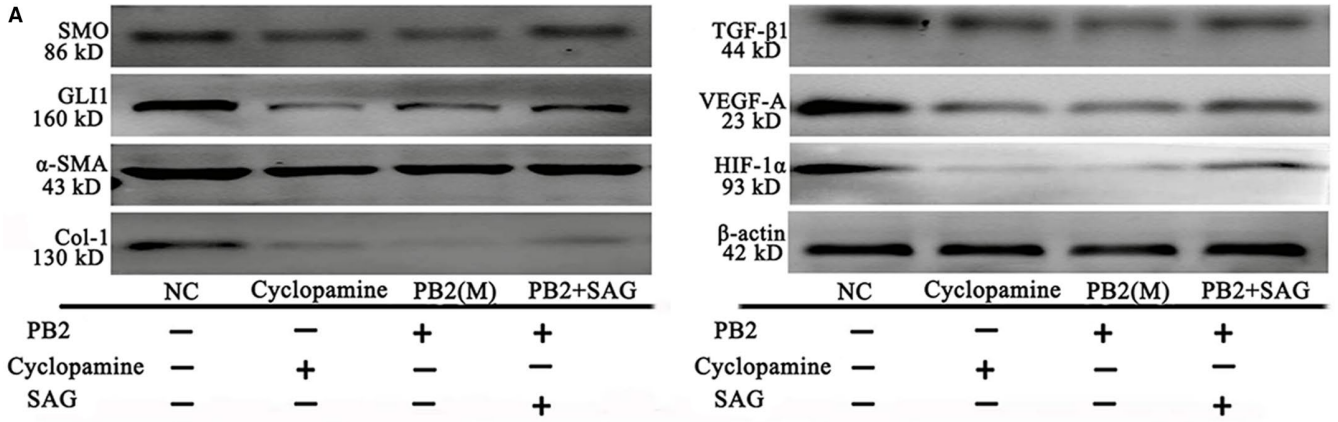
3.6 | PB2 reverses liver fibrosis by down-regulating the Hh pathway in vivo and in vitro

To further determine the molecular mechanism of PB2 in liver fibrosis, the Hh pathway aroused our attention. SMO and GLI1 are two important molecules in the Hh pathway. In the CCl4-induced liver fibrosis model in mice, IHC staining showed that in the vehicle group there was minimal expression of SMO and GLI1 in normal liver tissues, but increased expression in the CCl4 group (Figure 5A). In the PB2-treated groups, expression of SMO and GLI1 was decreased. The Western blot results were consistent with the IHC staining results (Figures 5B,C). HIF-1 α is not only a target gene of the Hh pathway, but a neovascularization-driven factor, playing a role in angiogenesis and liver injury during liver fibrosis.^{6,32} The IHC staining and Western blot results revealed that there was high expression of HIF-1 α in fibrotic liver tissues, and the expression could be inhibited by PB2 (Figure 5A-C).

Moreover, we used the Hh pathway inhibitor cyclopamine to compare the role of PB2 and cyclopamine in vivo. The results in Figure 5C demonstrated that both PB2 and cyclopamine can relieve the pathological injuries and collagen deposition in liver tissues, and if treated with both PB2 and cyclopamine, the improvement was more effective than mono-treatment. The Western blotting analysis of α -SMA, VEGF-A and GLI1 in liver tissues also revealed that PB2 and cyclopamine co-treatment was better to relief HSCs activation, angiogenesis and the Hh pathway than the mono-treatment. These results indicated that PB2 was effective to reduced liver fibrosis as Hh inhibitor cyclopamine did, and PB2 and cyclopamine co-treatment exhibited a better effect than mono-treatment.

Immunofluorescence staining of GLI1 was positive in the cytoplasm and nuclei of LX2 cells, which indicated that the Hh pathway was activated in HSCs (Figure 6D); however, if the LX2 cells were treated with PB2, the expression and translocation of GLI1 from the cytoplasm to the nucleus was inhibited. To verify whether or not the Hh pathway was the target of PB2 action, we used the cyclopamine (a SMO inhibitor) and SAG (a SMO agonist). As shown in Figure 6A-C, the Western blot and qRT-PCR results revealed that the expression of SMO and GLI1 was high in the NC group. In the cyclopamine group, if the LX2 cells were treated with a Hh pathway inhibitor, the expression of SMO and Hh was dramatically reduced. In the PB2 (M) group, the inhibitory effects of PB2 on SMO and GLI1 were almost the same as cyclopamine, while the inhibition was significantly reversed by SAG. These findings demonstrated that the Hh pathway was the target action site of PB2 in liver fibrosis. The detection of α -SMA, Col-1, TGF- β 1, VEGF-A and HIF-1 α by Western blot and qRT-PCR also showed that by inhibiting the Hh pathway by cyclopamine, the activation and angiogenesis ability of LX2 cells were significantly

FIGURE 6 Effects of PB2 on the Hh pathway in LX2 cells. A, Effects of cyclopamine, PB2, and SAG on the Hh pathway, and the activation and angiogenesis ability of LX2 cells. B, The quantitative analysis of Western blot results. C, The levels of SMO, GLI1, α -SMA, Col-1 α 1, Col-1 α 2, TGF- β 1, VEGF-A and HIF-1 α mRNA in LX2 cells. D, IF staining of GLI1 in LX2 cells (original magnification, 400 \times). All of the experiments were repeated in triplicate. Data are presented as the mean \pm SD from three independent experiments. * Indicates $P < .05$ vs the NC group; # indicates $P < .05$ vs the L group; and † indicates $P < .05$ vs the M group



inhibited. Overall, these analyses confirmed that PB2 inhibited the Hh pathway to inhibit the activation, ECM production and angiogenesis ability of HSCs during liver fibrosis *in vivo* and *in vitro*.

4 | DISCUSSION

Liver fibrosis is a serious health problem worldwide because liver fibrosis can ultimately progress into end-stage liver cirrhosis and even HCC.³ The reversibility of liver fibrosis is commonly recognized if the fibrogenesis stimulus is removed.^{2,37} In many chronic liver diseases, however, the elimination of primary fibrogenesis factors cannot be eliminated. Various therapeutic measures have been developed to reverse liver fibrosis, such as immunosuppressants, anti-inflammatory agents, PPAR- γ agonists, pan-caspase inhibitors and Hh inhibitors.³⁷⁻⁴⁰

PB2 (epicatechin-(4h-8)-epicatechin), which is rich in grape seeds, apples and cacao beans, is well-known for its anti-inflammatory and anti-tumour properties.^{41,42} Previously, PB2 has been reported to protect against CCl₄-induced acute liver injury by suppressing the inflammatory response and apoptosis in liver tissues.⁴² There are no studies about the effects of PB2 on chronic liver injuries to date. Therefore, we used CCl₄ to induce a liver fibrosis murine model and examine the effects of PB2 on chronic liver injuries. The results in Figure 1 revealed that PB2 was safe for the long-term use in mice, and 50, 100 and 150 mg/kg could inhibit and even reverse the progression of liver fibrosis.

Liver fibrosis is characterized by the over-deposition of ECM, and the activation of HSCs by TGF- β 1, PDGF and EGF is the key link to the pathogenesis of liver fibrosis.^{5,43} In the normal liver, HSCs maintain the production and degradation of ECM to maintain the balance of ECM deposition; however, in liver fibrosis the excessive activation of qHSCs to aHSCs contributes to the over-deposition of ECM, especially collagen.^{3,4} The results in Figure 2 showed that the expression

of Col-1 is significantly inhibited by PB2, which further confirmed the protective effect of PB2 on liver fibrosis. Subsequently, we used a human immortal HSC cell line (LX2) to more thoroughly investigate the protective mechanism. We found that the proliferation and activation of LX2 cells were restrained by PB2, and ECM production of LX2 cells was also decreased. In addition, flow cytometry demonstrated that PB2 promotes apoptosis of LX2 cells. In summary, we showed that PB2 decreased the number of LX2 cells via inhibition of proliferation and induction of apoptosis, and inhibited the activation and ECM production ability of relict LX2 cells to exert an anti-fibrotic effect.

We also showed that PB2 ameliorated angiogenesis of HSCs *in vivo* and *in vitro*, which was reflected by the inhibition of VEGF-A expression and tubulogenesis ability of LX2 cells. Many studies have shown that angiogenesis is associated with fibrogenesis, and angiogenesis is thus a promising therapeutic target of liver fibrosis.^{44,45} There are close connections between the activation of HSCs and angiogenesis. First, aHSCs possess angiogenesis ability by secreting VEGF-A and angiopoietin 1, which can directly stimulate the sinus endothelial cells and provoke the formation and stability of neovascularity.^{33,46,47} VEGF-A can also provide positive feedback to promote the proliferation and activation of HSCs.⁴⁸ Second, angiogenesis is a hypoxia-stimulated process in liver fibrosis because the over-deposition of ECM disrupts the architecture and gives rise to tissue hypoxia.^{6,32} The aHSCs enhance the expression of HIF-1 α , leading to the transcription of an increase in angiogenesis genes.^{49,50} Third, the HSCs can also express lots of CXC chemokines, which can manipulate angiogenesis during initiation and progression of fibrogenesis.⁵¹ Fourth, HSCs can also regulate the blood flow of vessels to modulate hepatic microvascular dynamics.⁵² Fifth, angiogenesis during liver fibrosis is invalid blood vessels, which are deficient in improving but will accelerate tissue hypoxia. In contrast, the angiogenesis will exacerbate structure turbulence and hypoxia, which can promote activation and ECM

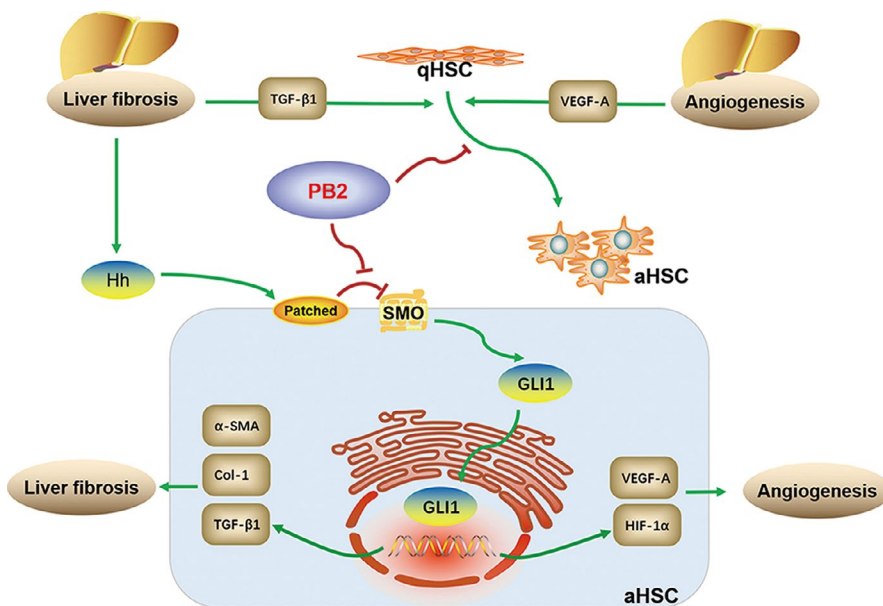


FIGURE 7 Mechanism of PB2 on the protective effect in liver fibrosis. Liver fibrosis is mainly initiated by the activation of HSCs. The injured liver tissues can release Hh ligands to activate the Hh pathway, leading to the activation of HSCs, ECM deposition and angiogenesis during liver fibrosis. In the current study, PB2 directly inhibited the Hh signalling pathway, therefore down-regulating the transcription of VEGF-A, HIF-1 α , α -SMA, Col-1 and TGF- β 1 in HSCs to suppress the activation, ECM production and angiogenesis of HSCs, leading to the reversal of liver fibrosis

production of HSCs.^{33,53} In the current study, PB2 inhibited the angiogenesis in LX2 cells and liver tissues, which also accounted for the anti-fibrotic effect of PB2 (Figure 7).

The precise action target of PB2 was further investigated. As reported, the Hh pathway plays an important role during liver fibrosis, including the activation, ECM secretion and metabolism of HSCs to control liver fibrosis.⁵⁴⁻⁵⁶ The Hh signalling pathway is initiated by the secretion of ligands (including sonic hedgehog [Shh], Indian hedgehog [Ihh] and desert hedgehog [Dhh]).⁵⁷ The HSCs are Hh-responsive cells and can receive the Hh ligands auto- or pan-secreted by injured hepatocytes, HSCs, liver progenitors and some types of resident lymphocytes, which can then interact with the receptor, Patched.^{19,42} Patched will eliminate the inhibitory effect on SMO, which will then promote the activation and nuclear translocation of the transcription factor, GLI1, resulting in the expression of Hh-target genes, such as VEGF-1, HIF-1 α , Gli1, SMO and Bcl-2.^{58,59} The Hh pathway also plays a role in angiogenesis in liver fibrosis, as well as hepatocarcinoma.⁶⁰ Therefore, in the current study we used the SMO inhibitor, cyclopamine, and the SMO agonist, SAG, to determine the role of PB2 on the Hh pathway in liver fibrosis. Indeed, PB2 possessed almost the same inhibitory effect on the Hh pathway as cyclopamine, and the inhibitory effect was reversed by SAG. These findings primarily indicated that the Hh pathway is the action target of PB2 on liver fibrosis. In addition, inhibition of the Hh pathway by cyclopamine and PB2 can inhibit the activation, ECM production and angiogenesis effect of HSCs, probably via the down-regulation of VEGF-A, HIF-1 α , α -SMA, Col-1 and TGF- β 1 transcription in LX2 cells.

In addition, because liver fibrosis may progress into liver cirrhosis and even hepatocarcinoma, and angiogenesis is a crucial characteristic of cancer, the anti-angiogenesis property of PB2 suggested a possible therapeutic role in hepatocarcinoma as well.

In conclusion, we confirmed that PB2 inhibited the Hh signalling pathway and therefore down-regulated the transcription of VEGF-A, HIF-1 α , α -SMA, Col-1 and TGF- β 1 in HSCs to suppress activation, ECM production and angiogenesis, thus reversing the progression of liver fibrosis.

ACKNOWLEDGEMENTS

This research was funded by Shanghai Natural Science Foundation (grant number: 19ZR1447700). We give thanks to all the staff in the Central Laboratory of Shanghai Tenth People's Hospital. And we thank International Science Editing (<http://www.international-scienceediting.com>) for editing this manuscript for us.

CONFLICT OF INTEREST

The authors confirm that there are no conflicts of interest.

AUTHOR CONTRIBUTIONS

J. Feng and J. Li contributed to the design of research; J. Feng, L. Wu, J. Ji and K. Chen performed the data analysis; J. Feng, Q. Yu,

S. Li and T. Liu helped perform the cellular experiments; J. Zhang, J. Chen and Y. Zhou helped perform the animal experiments; Y. Mao, F. Wang and W. Dai conducted some other experiments; J. Feng wrote the manuscript; X. Fan, J. Wu and Chuanyong Guo edited the manuscript.

DATA AVAILABILITY STATEMENT

The datasets generated during and/or analysed during the current study are available from the corresponding author on reasonable request.

ORCID

Chuanyong Guo  <https://orcid.org/0000-0002-6527-4673>

REFERENCES

1. Wang P, Koyama Y, Liu X, et al. Promising therapy candidates for liver fibrosis. *Front Physiol.* 2016;7:47.
2. Toosi AE. Liver fibrosis: causes and methods of assessment. A review. *Rom J Intern Med.* 2015;53:304-314.
3. Sun M, Kisseleva T. Reversibility of liver fibrosis. *Clin Res Hepatol Gastroenterol.* 2015;39(suppl 1):S60-S63.
4. Kisseleva T, Brenner DA. Mechanisms of fibrogenesis. *Exp Biol Med (Maywood).* 2008;233:109-122.
5. Hernandez-Gea V, Friedman SL. Pathogenesis of liver fibrosis. *Annu Rev Pathol.* 2011;6:425-456.
6. Zhang F, Hao M, Jin H, et al. Canonical hedgehog signalling regulates hepatic stellate cell-mediated angiogenesis in liver fibrosis. *Br J Pharmacol.* 2017;174:409-423.
7. Lee JS, Semela D, Iredale J, Shah VH. Sinusoidal remodeling and angiogenesis: a new function for the liver-specific pericyte? *Hepatology.* 2007;45:817-825.
8. Mejias M, Garcia-Pras E, Tiani C, Miquel R, Bosch J, Fernandez M. Beneficial effects of sorafenib on splanchnic, intrahepatic, and portocollateral circulations in portal hypertensive and cirrhotic rats. *Hepatology.* 2009;49:1245-1256.
9. Hennenberg M, Trebicka J, Stark C, Kohistani AZ, Heller J, Sauerbruch T. Sorafenib targets dysregulated Rho kinase expression and portal hypertension in rats with secondary biliary cirrhosis. *Br J Pharmacol.* 2009;157:258-270.
10. Feng J, Zhang XL, Li YY, Cui YY, Chen YH. *Pinus massoniana* bark extract: structure-activity relationship and biomedical potentials. *Am J Chin Med.* 2016;44:1559-1577.
11. Hammerstone JF, Lazarus SA, Mitchell AE, Rucker R, Schmitz HH. Identification of procyanidins in cocoa (*Theobroma cacao*) and chocolate using high-performance liquid chromatography/mass spectrometry. *J Agric Food Chem.* 1999;47:490-496.
12. Monagas M, Quintanilla-Lopez JE, Gomez-Cordoves C, Bartolome B, Lebron-Aguilar R. MALDI-TOF MS analysis of plant proanthocyanidins. *J Pharm Biomed Anal.* 2010;51:358-372.
13. Fine AM. Oligomeric proanthocyanidin complexes: history, structure, and phytopharmaceutical applications. *Altern Med Rev.* 2000;5:144-151.
14. Feng J, Wu L, Ji J, et al. PKM2 is the target of proanthocyanidin B2 during the inhibition of hepatocellular carcinoma. *J Exp Clin Cancer Res.* 2019;38:204.
15. Tyagi A, Raina K, Shrestha SP, et al. Procyanidin B2 3,3(=)-di-O-gallate, a biologically active constituent of grape seed extract,

- induces apoptosis in human prostate cancer cells via targeting NF-kappaB, Stat3, and AP1 transcription factors. *Nutr Cancer*. 2014;66:736-746.
16. Yang H, Xiao L, Yuan Y, et al. Procyanidin B2 inhibits NLRP3 inflammasome activation in human vascular endothelial cells. *Biochem Pharmacol*. 2014;92:599-606.
 17. Justino AB, Pereira MN, Peixoto LG, et al. Hepatoprotective properties of a polyphenol-enriched fraction from *Annona crassiflora* mart. fruit peel against diabetes-induced oxidative and nitrosative stress. *J Agric Food Chem*. 2017;65:4428-4438.
 18. Yang BY, Zhang XY, Guan SW, Hua ZC. Protective effect of procyanidin B2 against CCl4-induced acute liver injury in mice. *Molecules*. 2015;20:12250-12265.
 19. Choi SS, Omenetti A, Syn WK, Diehl AM. The role of Hedgehog signaling in fibrogenic liver repair. *Int J Biochem Cell Biol*. 2011;43:238-244.
 20. Yang JJ, Tao H, Li J. Hedgehog signaling pathway as key player in liver fibrosis: new insights and perspectives. *Expert Opin Ther Targets*. 2014;18:1011-1021.
 21. Bijlsma MF, Groot AP, Oduro JP, et al. Hypoxia induces a hedgehog response mediated by HIF-1alpha. *J Cell Mol Med*. 2009;13:2053-2060.
 22. Li J, Chen K, Li S, et al. Protective effect of fucoidan from *Fucus vesiculosus* on liver fibrosis via the TGF-beta1/Smad pathway-mediated inhibition of extracellular matrix and autophagy. *Drug Des Devel Ther*. 2016;10:619-630.
 23. Liu T, Xu L, Wang C, et al. Alleviation of hepatic fibrosis and autophagy via inhibition of transforming growth factor-beta1/Smads pathway through shikonin. *J Gastroenterol Hepatol*. 2019;34(1):263-276.
 24. Shen M, Chen K, Lu J, et al. Protective effect of astaxanthin on liver fibrosis through modulation of TGF-beta1 expression and autophagy. *Mediators Inflamm*. 2014;2014:954502.
 25. Feng J, Chen K, Xia Y, et al. Salidroside ameliorates autophagy and activation of hepatic stellate cells in mice via NF-kappaB and TGF-beta1/Smad3 pathways. *Drug Des Devel Ther*. 2018;12:1837-1853.
 26. Wu L, Zhang Q, Mo W, et al. Quercetin prevents hepatic fibrosis by inhibiting hepatic stellate cell activation and reducing autophagy via the TGF-beta1/Smads and PI3K/Akt pathways. *Sci Rep*. 2017;7:9289.
 27. Arensdorf AM, Dillard ME, Menke JM, Frank MW, Rock CO, Ogden SK. Sonic Hedgehog activates phospholipase a2 to enhance smoothed ciliary translocation. *Cell Rep*. 2017;19:2074-2087.
 28. Bragina O, Sergejeva S, Serg M, et al. Smoothed agonist augments proliferation and survival of neural cells. *Neurosci Lett*. 2010;482:81-85.
 29. Street JM, Souza AC, Alvarez-Prats A, et al. Automated quantification of renal fibrosis with Sirius Red and polarization contrast microscopy. *Physiol Rep*. 2014;2:e12088.
 30. Livak KJ, Schmittgen TD. Analysis of relative gene expression data using real-time quantitative PCR and the 2^{-Delta Delta C(T)} method. *Methods*. 2001;25:402-408.
 31. Zhan L, Yang Y, Ma TT, et al. Transient receptor potential vanilloid 4 inhibits rat HSC-T6 apoptosis through induction of autophagy. *Mol Cell Biochem*. 2015;402:9-22.
 32. Troeger JS, Schwabe RF. Hypoxia and hypoxia-inducible factor 1alpha: potential links between angiogenesis and fibrogenesis in hepatic stellate cells. *Liver Int*. 2011;31:143-145.
 33. Copple BL, Bai S, Burgoon LD, Moon JO. Hypoxia-inducible factor-1alpha regulates the expression of genes in hypoxic hepatic stellate cells important for collagen deposition and angiogenesis. *Liver Int*. 2011;31:230-244.
 34. Wang Z, Li J, Xiao W, Long J, Zhang H. The STAT3 inhibitor S31-201 suppresses fibrogenesis and angiogenesis in liver fibrosis. *Lab Invest*. 2018;98:1600-1613.
 35. Li S, Dai W, Mo W, et al. By inhibiting PFKFB3, aspirin overcomes sorafenib resistance in hepatocellular carcinoma. *Int J Cancer*. 2017;141:2571-2584.
 36. Li S, Li J, Dai W, et al. Genistein suppresses aerobic glycolysis and induces hepatocellular carcinoma cell death. *Br J Cancer*. 2017;117:1518-1528.
 37. Schuppan D. Liver fibrosis: common mechanisms and antifibrotic therapies. *Clin Res Hepatol Gastroenterol*. 2015;39(suppl 1):S51-S59.
 38. Zhang Y, Li Y, Zhang L, Li J, Zhu C. Mesenchymal stem cells: potential application for the treatment of hepatic cirrhosis. *Stem Cell Res Ther*. 2018;9:59.
 39. Lu X, Liu T, Chen K, et al. Isorhamnetin: a hepatoprotective flavonoid inhibits apoptosis and autophagy via P38/PPAR-alpha pathway in mice. *Biomed Pharmacother*. 2018;103:800-811.
 40. Wang W, Chen K, Xia Y, et al. The hepatoprotection by oleanolic acid preconditioning: focusing on PPARalpha activation. *PPAR Res*. 2018;2018:3180396.
 41. Keen CL. Chocolate: food as medicine/medicine as food. *J Am Coll Nutr*. 2001; 20:436S-439S; discussion:40S-42S.
 42. Chen Y, Choi SS, Michelotti GA, et al. Hedgehog controls hepatic stellate cell fate by regulating metabolism. *Gastroenterology*. 2012;143(1319-29):e11.
 43. Liu Y, Wang Z, Kwong SQ, et al. Inhibition of PDGF, TGF-beta, and Abl signaling and reduction of liver fibrosis by the small molecule Bcr-Abl tyrosine kinase antagonist Nilotinib. *J Hepatol*. 2011;55:612-625.
 44. Medina J, Arroyo AG, Sanchez-Madrid F, Moreno-Otero R. Angiogenesis in chronic inflammatory liver disease. *Hepatology*. 2004;39:1185-1195.
 45. Yoshiji H, Kuriyama S, Yoshii J, et al. Vascular endothelial growth factor and receptor interaction is a prerequisite for murine hepatic fibrogenesis. *Gut*. 2003;52:1347-1354.
 46. Elpek GO. Angiogenesis and liver fibrosis. *World J Hepatol*. 2015;7:377-391.
 47. Lai WK, Adams DH. Angiogenesis and chronic inflammation; the potential for novel therapeutic approaches in chronic liver disease. *J Hepatol*. 2005;42:7-11.
 48. Yin C, Evason KJ, Asahina K, Stainier DY. Hepatic stellate cells in liver development, regeneration, and cancer. *J Clin Invest*. 2013;123:1902-1910.
 49. Hickey MM, Simon MC. Regulation of angiogenesis by hypoxia and hypoxia-inducible factors. *Curr Top Dev Biol*. 2006;76:217-257.
 50. Nath B, Szabo G. Hypoxia and hypoxia inducible factors: diverse roles in liver diseases. *Hepatology*. 2012;55:622-633.
 51. Strieter RM, Burdick MD, Gomperts BN, Belperio JA, Keane MP. CXC chemokines in angiogenesis. *Cytokine Growth Factor Rev*. 2005;16:593-609.
 52. Coulon S, Heindryckx F, Geerts A, Van Steenkiste C, Colle I, Van Vlierberghe H. Angiogenesis in chronic liver disease and its complications. *Liver Int*. 2011;31:146-162.
 53. Berres ML, Koenen RR, Rueland A, et al. Antagonism of the chemokine Ccl5 ameliorates experimental liver fibrosis in mice. *J Clin Invest*. 2010;120:4129-4140.
 54. Choi SS, Omenetti A, Witek RP, et al. Hedgehog pathway activation and epithelial-to-mesenchymal transitions during myofibroblastic transformation of rat hepatic cells in culture and cirrhosis. *Am J Physiol Gastrointest Liver Physiol*. 2009;297:G1093-G1106.
 55. Witek RP, Yang L, Liu R, et al. Liver cell-derived microparticles activate hedgehog signaling and alter gene expression in hepatic endothelial cells. *Gastroenterology*. 2009;136(320-30):e2.
 56. Li T, Leng XS, Zhu JY, Wang G. Suppression of hedgehog signaling regulates hepatic stellate cell activation and collagen secretion. *Int J Clin Exp Pathol*. 2015;8:14574-14579.

57. Pimentel A, Velez M, Barahona LJ, Swords R, Lekakis L. New prospects for drug development: the hedgehog pathway revealed. Focus on hematologic malignancies. *Future Oncol.* 2013;9:681-697.
58. Ruch JM, Kim EJ. Hedgehog signaling pathway and cancer therapeutics: progress to date. *Drugs.* 2013;73:613-623.
59. McMillan R, Matsui W. Molecular pathways: the hedgehog signaling pathway in cancer. *Clin Cancer Res.* 2012;18:4883-4888.
60. Vokes SA, Yatskievych TA, Heimark RL, et al. Hedgehog signaling is essential for endothelial tube formation during vasculogenesis. *Development.* 2004;131:4371-4380.

How to cite this article: Feng J, Wang C, Liu T, et al. Procyanidin B2 inhibits the activation of hepatic stellate cells and angiogenesis via the Hedgehog pathway during liver fibrosis. *J Cell Mol Med.* 2019;23:6479-6493. <https://doi.org/10.1111/jcmm.14543>